Atmospheric Chemistry of CH 3 O(CF 2 CF 2 O) n CH 3 (n = 1−3): Kinetics and Mechanism of Oxidation Initiated by Cl Atoms and OH Radicals, IR Spectra, and Global Warming Potentials

ARTICLE *in* THE JOURNAL OF PHYSICAL CHEMISTRY A · MARCH 2004

Impact Factor: 2.69 · DOI: 10.1021/jp036615a

12 AUTHORS, INCLUDING:

Vito Librando
University of Catania
144 PUBLICATIONS **1,259** CITATIONS
SEE PROFILE

Jens Hjorth
European Commission
115 PUBLICATIONS **3,233** CITATIONS
SEE PROFILE

G. Marchionni
Solvay
60 PUBLICATIONS **572** CITATIONS
SEE PROFILE

Ole John Nielsen
University of Copenhagen
263 PUBLICATIONS **4,912** CITATIONS
SEE PROFILE

Atmospheric Chemistry of $CH_3O(CF_2CF_2O)_nCH_3$ ($n = 1-3$): Kinetics and Mechanism of Oxidation Initiated by Cl Atoms and OH Radicals, IR Spectra, and Global Warming Potentials

M. P. Sulbaek Andersen, M. D. Hurley, and T. J. Wallington*

Ford Research and Advanced Engineering, SRL-3083, Ford Motor Company, Dearborn, P.O. Box 2053, Michigan 48121-2053

F. Blandini,[†,‡] N. R. Jensen,*[,†] V. Librando,[‡] and J. Hjorth[†]

EC-Joint Research Centre, Institute for Environment and Sustainability, TP 290, I-21020 Ispra (VA), Italy, and Chemistry Department, University of Catania, Viale Doria 6, I-95127 Catania, Italy

G. Marchionni, M. Avataneo, and M. Visca

Solvay Solexis, Via S. Pietro 50, I-20021 Bollate (MI), Italy

F. M. Nicolaisen and O. J. Nielsen

Department of Chemistry, University of Copenhagen, Universitetsparken 5, DK-2100 Copenhagen, Denmark

Received: September 2, 2003; In Final Form: November 21, 2003

Smog chambers equipped with FTIR spectrometers were used to study the Cl atom and OH radical initiated oxidation of $CH_3O(CF_2CF_2O)_nCH_3$ ($n = 1-3$) in 720 ± 20 Torr of air at 296 ± 3 K. Relative rate techniques were used to measure $k(Cl + CH_3O(CF_2CF_2O)_nCH_3) = (3.7 \pm 0.7) \times 10^{-13}$ and $k(OH + CH_3O(CF_2CF_2O)_nCH_3) = (2.9 \pm 0.5) \times 10^{-14}$ cm^3 molecule^{-1} s^{-1} leading to an estimated atmospheric lifetime of 2 years for $CH_3O(CF_2CF_2O)_nCH_3$. The Cl initiated oxidation of $CH_3O(CF_2CF_2O)_nCH_3$ in air diluent gives $CH_3O(CF_2CF_2O)_nC(O)H$ in a yield which is indistinguishable from 100%. Further oxidation leads to the diformate, $H(O)CO(CF_2CF_2O)_nC(O)H$. A rate constant of $k(Cl + CH_3O(CF_2CF_2O)_nCHO) = (1.81 \pm 0.36) \times 10^{-13}$ cm^3 molecule^{-1} s^{-1} was determined. Quantitative infrared spectra for $CH_3O(CF_2CF_2O)_nCH_3$ ($n = 1-3$) were recorded and used to estimate halocarbon global warming potentials of 0.051, 0.058, and 0.055 (100 year time horizon, relative to CFC-11) for $CH_3OCF_2CF_2OCH_3$, $CH_3O(CF_2CF_2O)_2CH_3$, and $CH_3O(CF_2CF_2O)_3CH_3$, respectively. Results are discussed with respect to the atmospheric chemistry of hydrofluoropolyethers (HFPEs).

1. Introduction

Recognition of the adverse environmental impact of chlorofluorocarbon (CFC) release into the atmosphere[1,2] has led to an international effort to replace CFCs with environmentally acceptable alternatives. A new class of hydrofluoropolyethers (HFPEs) having the structure $CH_3O(CF_2CF_2O)_n(CF_2O)_mCH_3$ has been developed as potential CFC replacements.[3−6] HFPEs do not contain chlorine and hence do not contribute to chlorine based catalytic destruction of stratospheric ozone. The incorporation of $-OCH_3$ groups provides reactive sites for OH radical attack which limit the atmospheric lifetime and hence global warming potential of these compounds.

As with other fluorinated compounds, HFPEs have high thermal and chemical stability and excellent heat exchange characteristics. In addition, due to the presence of the $-OCH_3$ groups, HFPEs are partially miscible with organic liquids. The thermodynamic and physical properties of the HFPEs considered here are reported and compared to other hydrofluoropolyethers and to hydrofluoroethers (HFEs) elsewhere.[7] HFPEs may find significant commercial use in a variety of applications. Prior to large-scale industrial use an assessment of the atmospheric chemistry, and hence environmental impact, of these compounds is needed.

Atmospheric oxidation of $CH_3O(CF_2CF_2O)_nCH_3$ will be initiated by reaction with OH radicals

$$CH_3O(CF_2CF_2O)_nCH_3 + OH \rightarrow CH_3O(CF_2CF_2O)_nC(\cdot)H_2 + H_2O \quad (1)$$

$$CH_3O(CF_2CF_2O)_nC(\cdot)H_2 + O_2 + M \rightarrow CH_3O(CF_2CF_2O)_nCH_2O_2(\cdot) + M \quad (2)$$

By analogy to other peroxy radicals,[8,9] the $CH_3O(CF_2CF_2O)_nCH_2O_2(\cdot)$ radicals are expected to react with NO, NO_2, HO_2, and other peroxy radicals under atmospheric conditions:

$$CH_3O(CF_2CF_2O)_nCH_2O_2(\cdot) + NO \rightarrow CH_3O(CF_2CF_2O)_nCH_2O(\cdot) + NO_2 \quad (3a)$$

$$CH_3O(CF_2CF_2O)_nCH_2O_2(\cdot) + NO + M \rightarrow CH_3O(CF_2CF_2O)_nCH_2ONO_2 + M \quad (3b)$$

* To whom correspondence should be addressed. E-mail: twalling@ford.com (T.J.W.); niels.jensen@jrc.it (N.R.J.).
† EC-Joint Research Centre.
‡ University of Catania.

10.1021/jp036615a CCC: $27.50
Published on Web 02/25/2004

$$CH_3O(CF_2CF_2O)_nCH_2O_2(\cdot) + NO_2 + M \leftrightarrow CH_3O(CF_2CF_2O)_nCH_2O_2NO_2 + M \quad (4)$$

$$CH_3O(CF_2CF_2O)_nCH_2O_2(\cdot) + HO_2 \rightarrow \text{products} \quad (5)$$

$$CH_3O(CF_2CF_2O)_nCH_2O_2(\cdot) + R'O_2(\cdot) \rightarrow \text{products} \quad (6)$$

To improve our knowledge of the atmospheric chemistry of HFPEs in general, and $CH_3O(CF_2CF_2O)_nCH_3$ in particular, samples of $CH_3OCF_2CF_2OCH_3$ (bp = 92 °C), $CH_3O(CF_2CF_2O)_2CH_3$ (bp = 135 °C), and $CH_3O(CF_2CF_2O)_3CH_3$ (bp = 161 °C) were prepared at Solvay Solexis. The kinetics of reaction 1 and the fate of the alkoxy radical $CH_3O(CF_2CF_2O)_nCH_2O(\cdot)$ produced in reaction 3a were determined using Fourier transform infrared (FTIR) spectrometers coupled to smog chambers at Ford Motor Company and at JRC−Ispra. IR spectra of $CH_3O(CF_2CF_2O)_nCH_3$ ($n = 1-3$) were measured at the University of Copenhagen and used to calculate global warming potentials for these species. We report herein the results of the first study of the atmospheric chemistry of $CH_3O(CF_2CF_2O)_nCH_3$.

2. Experimental Section

The experimental systems and procedures used in this work are described in detail elsewhere.[10,11] Samples of $CH_3OCF_2CF_2OCH_3$, $CH_3O(CF_2CF_2O)_2CH_3$, and $CH_3O(CF_2CF_2O)_3CH_3$ were supplied by Solvay Solexis at purities >99.5%. Unless stated otherwise, all uncertainties quoted in the present manuscript are 2 standard deviations from regression analyses. Standard error propagation methods were used to calculate combined uncertainties where appropriate.

2.1. Synthesis of $CH_3O(CF_2CF_2O)_nCH_3$ ($n = 1-3$). The synthesis of $CH_3O(CF_2CF_2O)_nCH_3$ is described in detail elsewhere.[3−6] The starting material is tetrafluoroethylene, which is reacted with O_2 at high pressure in the presence of elemental F_2 to give a mixture of perfluorinated polyethers. Reaction of the peroxidic polyethers with hydrogen over a suitable catalyst converts the peroxy bridges to acyl fluoride functional groups. The $-OCF_2C(O)F$ end groups are then converted into $-O-CH_3$ groups by reaction with an alkaline metal fluoride in an aprotic polar solvent (generally diglyme) in the presence of a methyl group carrying molecule. Finally, multiple fractional distillation is used to provide pure (>99.5%) samples of $CH_3O(CF_2CF_2O)_nCH_3$ ($n = 1-3$).

2.2. FTIR−Smog Chamber System at Ford Motor Co. All experiments were performed in a 140-liter Pyrex reactor interfaced to a Mattson Sirus 100 FTIR spectrometer.[10] The reactor was surrounded by 22 fluorescent blacklamps (GE F40BLB) which were used to photochemically initiate the experiments.

Cl atoms were generated by photolysis of Cl_2:

$$Cl_2 \xrightarrow{h\nu} 2Cl \quad (7)$$

OH radicals were generated by UV irradiation of CH_3ONO/NO/air mixtures:

$$CH_3ONO \xrightarrow{h\nu} CH_3O + NO \quad (8)$$

$$CH_3O + O_2 \rightarrow HCHO + HO_2 \quad (9)$$

$$HO_2 + NO \rightarrow OH + NO_2 \quad (10)$$

Reactant and product concentrations were monitored using in situ Fourier transform infrared spectroscopy. IR spectra were derived from 32 coadded interferograms with a spectral resolution of 0.25 cm^{-1} and an analytical path length of 27.1 m. Reference spectra were acquired by expanding known volumes of authentic reference compounds into the chamber.

Experiments were performed at 296 ± 3 K in 700 Torr of air diluent. All reagents except CH_3ONO were obtained from commercial sources at purities >99%. Samples of $CH_3O(CF_2CF_2O)_nCH_3$ were subjected to freeze−pump−thaw cycling before use. Ultrahigh purity nitrogen and synthetic air diluent gases were used as received. All other commercial samples were used without further purification. CH_3ONO was prepared by the dropwise addition of concentrated H_2SO_4 to a saturated solution of $NaNO_2$ in methanol and was devoid of any detectable impurities using FTIR analysis.

In smog chamber experiments, unwanted loss of reactants, reference compounds, and products via photolysis, chemistry occurring in the dark, and heterogeneous reactions have to be considered. Control experiments were performed in which reactant and product mixtures obtained after UV irradiation were allowed to stand in the dark in the chamber for 30 min. There was no observable (<2%) loss of reactants or products, showing that heterogeneous reactions in the dark are not a significant complication in the present experiments. Analysis of the IR spectra was achieved through a process of spectral stripping in which small fractions of the reference spectrum were subtracted incrementally from the sample spectrum.

The relative rate method is a well established and widely used procedure for measuring the reactivity of Cl atoms and OH radicals with organic compounds.[12] Kinetic data are derived by monitoring the loss of a reactant compound ($CH_3O(CF_2CF_2O)_nCH_3$ in the present work) relative to one or more reference compounds. The decays of the reactant and reference are then plotted using the expression:

$$Ln\left(\frac{[\text{reactant}]_{t_0}}{[\text{reactant}]_t}\right) = \frac{k_{\text{reactant}}}{k_{\text{reference}}} Ln\left(\frac{[\text{reference}]_{t_0}}{[\text{reference}]_t}\right)$$

where $[\text{reactant}]_{t0}$, $[\text{reactant}]_t$, $[\text{reference}]_{t0}$, and $[\text{reference}]_t$ are the concentrations of reactant and reference at times "t_0" and "t" and k_{reactant} and $k_{\text{reference}}$ are the rate constants for reactions of Cl atoms or OH radicals with the reactant and reference.

Photolysis of CH_3ONO is the most convenient and widely used source of OH radicals in relative rate studies. However, the use of CH_3ONO is not well suited to the study of less reactive compounds because CH_3ONO itself reacts with OH at a moderate rate (approximately 3×10^{-13} cm^3 $molecule^{-1}$ s^{-1} [13]), scavenges OH radicals and makes loss of the less reactive compound (e.g., $CH_3O(CF_2CF_2O)_nCH_3$) small and difficult to measure. In the present work, we have employed a variation of the typical relative rate method in which the loss of the reactant ($CH_3O(CF_2CF_2O)_nCH_3$) was monitored indirectly by observing the formation of its oxidation product ($CH_3O(CF_2CF_2O)_nC(O)H$). High initial concentrations of the HFPE (47−80 mTorr) were used to facilitate monitoring the $CH_3O(CF_2CF_2O)_nC(O)H$ product resulting from small (<1%) consumptions of the HFPE.

2.3. Smog Chamber System at JRC, Ispra. All investigations at Ispra were performed in a 480 L cylindrical Teflon-coated evacuable glass reaction chamber. A multiple reflection White-type mirror system was installed in the reactor, adjusted to give a total optical path length of 81.24 m, and coupled to a Bruker IFS 113 V FT-IR spectrometer for on-line infrared spectroscopy. Spectra were obtained by co-adding 20−40 scans recorded at 1 cm^{-1} instrumental resolution in the range from 600 to 4000 cm^{-1}. The reactants were mixed in synthetic air at 296 ± 3 K and 740 ± 5 Torr total pressure.

Cl atoms were produced by photolysis of Cl_2. OH was produced by photolysis of CH_3ONO in the presence of NO. The source of UV radiation was 18 UV and visible lamps (λ = 300−500 nm, maximum emittance at λ = 370 nm) surrounding the chamber. Rate constants were determined using relative rate methods (see section 2.2). Infrared spectra of $CH_3O(CF_2CF_2O)_n$-CH_3 (n = 1−3) in one atmosphere of air at room temperature were recorded in the region 600−4000 cm^{-1} using a Bruker IFS 113v with a nominal spectral resolution of 1 cm^{-1}. Measured integrated band intensities are given in Table 1.

Chemicals used in this investigation were: $CH_3O(CF_2CF_2O)_n$-CH_3 (> 99.5%, Solvay Solexis), Cl_2 (99.5%, Aldrich), CH_4 (> 99.5%, UCAR), CH_3Cl (> 99.5%, UCAR), and C_2H_4 (99.5%, Aldrich).

2.4. Copenhagen Set Up/Global Warming Calculations (GWPs). Infrared spectra of $CH_3O(CF_2CF_2O)_nCH_3$ (n = 1−3) were recorded at the University of Copenhagen using a BRUKER FT-IR spectrometer (FS HR-120), a globar source, and a DTGS detector. Spectra in the 500−2000 cm^{-1} region (mid infrared, MIR) were recorded using a KBr beam splitter and a 10.0 cm glass cell with KBr windows. Spectra in the 150−650 cm^{-1} region (far-infrared, FIR) were recorded using a 3.5 micron Mylar beam splitter and a 17.3 cm quartz cell with polyethylene (PET) windows. For the far-IR spectra, the cell was placed inside the instrument (in a vacuum). Background and sample spectra were recorded with a resolution of 0.5 cm^{-1}. The far-IR spectra and the MIR spectra overlap in the region 500−650 cm^{-1} providing an opportunity to check the internal consistency of the results; in all cases, the spectra agreed within the experimental uncertainties.

Sample handling was performed using a vacuum system made of glass with Teflon stopcocks. The system was evacuated using a turbo pump and the pressure was measured using a ceramic capacitance manometer (MKS Instruments, range 10 Torr). The accuracy of the pressure readings was better than 0.05 Torr. The HFPE pressures used were between 1.5 and 7 Torr (highest for the FIR-spectra). The absorption scaled linearly with the sample concentration. The spectra were recorded at 296 ± 1 K in the absence of added diluent gas. Such spectra acquired at room temperature should be adequate to estimate the instantaneous forcings of these molecules.[14] The accuracy of the resulting absorption cross sections is estimated to be 5%. The procedure outlined by Pinnock et al.[14] was used to estimate instantaneous forcings and global warming potentials (GWPs) of the compounds (see appendix).

3. Results

3.1. Relative Rate Study of $k(Cl + CH_3O(CF_2CF_2O)_nCH_3)$. The kinetics of reaction 11 were measured relative to reactions 12 and 13

$$CH_3O(CF_2CF_2O)_nCH_3 + Cl \rightarrow CH_3O(CF_2CF_2O)_nCH_2(\cdot) + HCl \quad (11)$$

$$CH_4 + Cl \rightarrow \text{products} \quad (12)$$

$$CH_3Cl + Cl \rightarrow \text{products} \quad (13)$$

The initial concentrations were 3.7−11 mTorr $CH_3O(CF_2$-$CF_2O)_nCH_3$, 104−182 mTorr Cl_2, and either 3.8−15.2 mTorr CH_3Cl or 3.8−15.2 mTorr CH_4 in 700 Torr of air diluent. Experiments employing $CH_3OCF_2CF_2OCH_3$ were performed at Ispra, whereas those using the longer chain $CH_3O(CF_2CF_2O)_2$-CH_3 and $CH_3O(CF_2CF_2O)_3CH_3$ compounds were performed at Ford. The observed loss of $CH_3O(CF_2CF_2O)_nCH_3$ versus those of the reference compounds in the presence of Cl atoms is shown in Figure 1. As seen from Figure 1, there was no discernible effect of the chain length (n = 1−3) on the reactivity of Cl atoms toward $CH_3O(CF_2CF_2O)_nCH_3$. Linear least-squares analysis of the data in Figure 1 gives $k_{11}/k_{12} = 3.36 \pm 0.32$ and $k_{11}/k_{13} = 0.823 \pm 0.083$. Using $k_{12} = 1.0 \times 10^{-13}$ and $k_{13} = 4.8 \times 10^{-13}$,[15] we derive $k_{11} = (3.36 \pm 0.32) \times 10^{-13}$ and $(3.95 \pm 0.40) \times 10^{-13}$ cm^3 $molecule^{-1}$ s^{-1}. We choose to cite a final value for k_{11}, which is the average of the two determinations with error limits which encompass the extremes of the individual determinations. Hence, $k_{11} = (3.7 \pm 0.7) \times 10^{-13}$ cm^3 $molecule^{-1}$ s^{-1}.

TABLE 1: Integrated Band Intensities over the Region 1060−1360 cm^{-1} (Units of 10^{-16} cm $molecule^{-1}$, Base e) at 296 K

compound	Ispra[a]	Copenhagen[b]	Ford[c]
$CH_3O(CF_2CF_2O)_1CH_3$	2.62 ± 0.26	2.24 ± 0.11	2.34 ± 0.12
$CH_3O(CF_2CF_2O)_2CH_3$	4.40 ± 0.44	4.51 ± 0.23	4.70 ± 0.24
$CH_3O(CF_2CF_2O)_3CH_3$	7.00 ± 0.70	6.88 ± 0.35	6.89 ± 0.34

[a] Measured in 740 Torr total pressure of air diluent. [b] No diluent used (see section 2.4). [c] Measured in 700 Torr total pressure of air diluent.

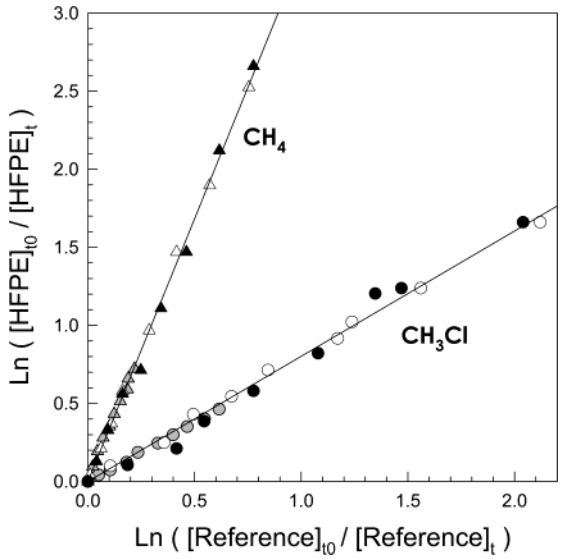

Figure 1. Decay of $CH_3O(CF_2CF_2O)_3CH_3$ (solid symbols), $CH_3O(CF_2$-$CF_2O)_2CH_3$ (open symbols), and $CH_3OCF_2CF_2OCH_3$ (gray symbols) versus CH_4 (triangles) and CH_3Cl (circles) in the presence of Cl atoms in 700 Torr of air diluent at 296 ± 3 K.

We find that $CH_3OCF_2CF_2OCH_3$, $CH_3O(CF_2CF_2O)_2CH_3$, and $CH_3O(CF_2CF_2O)_3CH_3$ have indistinguishable reactivities toward Cl atoms. This seems reasonable based upon expectations that the $-(CF_2CF_2O)_n-$ group will not react with Cl atoms, and that its influence on the reactivity of the methyl groups will not change markedly upon increasing "n" from 1 to 3. Hence, the results presented herein can be generalized to $k_{11} = (3.7 \pm 0.5) \times 10^{-13}$ cm^3 $molecule^{-1}$ s^{-1} for $n \geq 1$. Results obtained for other hydrofluoroethers are $k(Cl + CF_3OCH_3) = (1.4 \pm 0.2) \times 10^{-13}$ [16] and $k(Cl + C_4F_9OCH_3) = (9.7 \pm 1.4) \times 10^{-14}$ cm^3 $molecule^{-1}$ s^{-1}.[17] Reaction of these HFEs with Cl atoms occurs at the terminal CH_3 group. The reactivity of Cl atoms toward the methyl groups in $CH_3O(CF_2CF_2O)_nCH_3$ appears to be a factor of 1−2 larger than that of the methyl group in CF_3-OCH_3 and $C_4F_9OCH_3$.

3.2. Atmospheric Fate of $CH_3O(CF_2CF_2O)_nCH_2O(\cdot)$ Radicals. The atmospheric fate of $CH_3O(CF_2CF_2O)_nCH_2O(\cdot)$ radicals was studied using the FTIR-smog chamber system at Ford Motor

Company.[10] Experiments were performed using UV irradiation of $CH_3O(CF_2CF_2O)_nCH_3/Cl_2$/air mixtures with, and without, added NO. In these experiments $CH_3O(CF_2CF_2O)_nCH_2O(\cdot)$ radicals were formed either by reaction 14a or 3a

$$CH_3O(CF_2CF_2O)_nCH_2O_2(\cdot) + CH_3O(CF_2CF_2O)_nCH_2O_2(\cdot) \rightarrow 2\ CH_3O(CF_2CF_2O)_nCH_2O(\cdot) + O_2 \quad (14a)$$

$$CH_3O(CF_2CF_2O)_nCH_2O_2(\cdot) + CH_3O(CF_2CF_2O)_nCH_2O_2(\cdot) \rightarrow CH_3O(CF_2CF_2O)_nC(O)H + CH_3O(CF_2CF_2O)_nCH_2OH + O_2 \quad (14b)$$

$$CH_3O(CF_2CF_2O)_nCH_2O_2(\cdot) + NO \rightarrow CH_3O(CF_2CF_2O)_nCH_2O(\cdot) + NO_2 \quad (3a)$$

$$CH_3O(CF_2CF_2O)_nCH_2O_2(\cdot) + NO + M \rightarrow CH_3O(CF_2CF_2O)_nCH_2ONO_2 + M \quad (3b)$$

The $CH_3O(CF_2CF_2O)_nCH_2O(\cdot)$ radicals formed in reactions 14a and 3a are expected to undergo either reaction 15 or 16

$$CH_3O(CF_2CF_2O)_nCH_2O(\cdot) + O_2 \rightarrow CH_3O(CF_2CF_2O)_nC(O)H + HO_2 \quad (15)$$

$$CH_3O(CF_2CF_2O)_nCH_2O(\cdot) + M \rightarrow CH_3O(CF_2CF_2O)_n(\cdot) + HCHO + M \quad (16)$$

reaction 15 gives the formate, $CH_3O(CF_2CF_2O)_nC(O)H$, whereas the unimolecular decomposition reaction 16 gives an alkoxy radical which will further decompose and initiate a sequence of reactions "unzipping" the radical.[17] In the case of $CH_3O(CF_2CF_2O)_3(\cdot)$, the reaction sequence in air would lead to production of six COF_2 molecules and one HCHO molecule. COF_2 is easily detectable by its absorption features at 774 and 1850−2000 cm^{-1} and is a convenient marker for the importance of reaction 16.

In all of the experiments conducted here (with and without added NO), formation of COF_2 was only detectable for large consumptions (>30%) of the HFPE. In contrast, even for small (<2%) conversions of the parent HFPE, characteristic carbonyl absorption features were readily observed at 1792−1830 cm^{-1} (see panel B in Figures 2 and 3) which we ascribe to the formate $CH_3O(CF_2CF_2O)_nC(O)H$. We conclude that reaction 15 is the dominant loss mechanism of $CH_3O(CF_2CF_2O)_nCH_2O(\cdot)$ radicals in the system. From the absence of COF_2 for small conversions of HFPE and assuming that reaction 16 will lead to "unzipping" of the radical into COF_2, we derive an upper limit of $k_{16}/k_{15} < 1.3 \times 10^{16}$ cm^{-3} molecule. In one atmosphere of air at 296 K, the O_2 concentration is 5.2×10^{18} molecule cm^{-3}, and >97% of $CH_3O(CF_2CF_2O)_nCH_2O(\cdot)$ radicals will undergo reaction with O_2, whereas <3% will undergo decomposition via reaction 16. In the atmosphere, the temperature is generally lower than that in our chamber experiments. Reaction 16 is a unimolecular decomposition and will slow more than reaction 15 as the temperature is decreased. We conclude that the sole atmospheric fate of $CH_3O(CF_2CF_2O)_nCH_2O(\cdot)$ radicals is reaction with O_2 to give the corresponding formate.

Following the irradiation of HFPE/Cl_2/air mixtures, the concentrations of the formates were observed to increase linearly with loss of HFPE up until about 15% loss of the parent HFPE. For >60% conversions of HFPE, the intensity of the observed IR features attributed to the formate reached a maximum and then decreased. As the IR features attributed to the formate decreased, a new set of IR features (see panel C in Figures 2 and 3) was observed. We ascribe this behavior to reaction of Cl atoms with the methyl group in the formate, $CH_3O(CF_2CF_2O)_nC(O)H$, to form the diformate, $H(O)CO(CF_2CF_2O)_nC(O)H$. The yield of the diformate also followed a pattern of initial increase followed by a plateau and decrease, which we ascribe again to reaction with Cl atoms. Loss of $H(O)CO(CF_2CF_2O)_nC(O)H$ was accompanied by the formation of COF_2 in the system. Figures 2 and 3 show IR spectra of these products formed during the Cl initiated oxidation of $CH_3O(CF_2CF_2O)_2CH_3$ and $CH_3O(CF_2CF_2O)_3CH_3$, respectively. The presence of two bands in the carbonyl stretch region for the perfluoro alkyl formates is caused by syn and anti conformations. Ab initio calculations have shown[17] that the low- and high-frequency bands can be assigned to the syn and anti conformers, respectively.

By monitoring the formation and subsequent loss of the formate, $CH_3O(CF_2CF_2O)_nC(O)H$, as a function of the fractional conversion of $CH_3O(CF_2CF_2O)_nCH_3$, we can establish the rate constant of the reaction of Cl atoms with the formate. The relevant reactions are

$$CH_3O(CF_2CF_2O)_nCH_3 + Cl \rightarrow \alpha\ CH_3O(CF_2CF_2O)_nC(O)H + \text{other products} \quad (17)$$

$$CH_3O(CF_2CF_2O)_nC(O)H + Cl \rightarrow \text{products} \quad (18)$$

Reaction mixtures consisted of 3.3−38 mTorr $CH_3O(CF_2CF_2O)_nCH_3$ and 130−140 mTorr Cl_2 in 700 Torr air diluent. As shown elsewhere[18] the appropriate rate equations can be solved analytically to relate the amount of $CH_3O(CF_2CF_2O)_nC(O)H$ at any time t to the corresponding conversion of $CH_3O(CF_2CF_2O)_nCH_3$ as a function of the yield of the formate, α, and the rate constant ratio k_{18}/k_{17}, where k_{17} and k_{18} are the bimolecular rate constants of reactions 17 and 18, respectively. Thus

$$\frac{[CH_3O(CF_2CF_2O)_nC(O)H]_t}{[CH_3O(CF_2CF_2O)_nCH_3]_{t_0}} = \frac{\alpha}{1-\frac{k_{18}}{k_{17}}} \times (1-x) \times [(1-x)^{\{k_{18}/k_{17}-1\}} - 1] \quad \text{(i)}$$

where x is defined as

$$x \equiv \frac{\Delta[CH_3O(CF_2CF_2O)_nCH_3]_t}{[CH_3O(CF_2CF_2O)_nCH_3]_{t_0}}$$

As described above, there was no evidence for loss of $CH_3O(CF_2CF_2O)_nCH_2O(\cdot)$ radicals by any process other than reaction with O_2, and hence, we assume $\alpha = 1$. On this basis absolute calibrations were derived for the IR spectra of the formates (see panel B in Figures 2 and 3). Figure 4 shows plots of $[CH_3O(CF_2CF_2O)_nC(O)H]_t / [CH_3O(CF_2CF_2O)_nCH_3]_{t_0}$ vs $\Delta[CH_3O(CF_2CF_2O)_nCH_3]_t/[CH_3O(CF_2CF_2O)_nCH_3]_{t_0}$. There was no discernible effect of variation of $[CH_3O(CF_2CF_2O)_nCH_3]_{t_0}$ or $[Cl_2]_{t_0}$ over a factor of 2. Using nonlinear fits of expression (i) to the experimental data in Figure 4 gave values of k_{18}/k_{17} for $CH_3O(CF_2CF_2O)_2CH_3$ and $CH_3O(CF_2CF_2O)_3CH_3$ which were indistinguishable. The fits to the $CH_3O(CF_2CF_2O)_2CH_3$ and $CH_3O(CF_2CF_2O)_3CH_3$ data in Figure 4 are shown as dashed and dotted lines, respectively. A fit of expression (i) to the

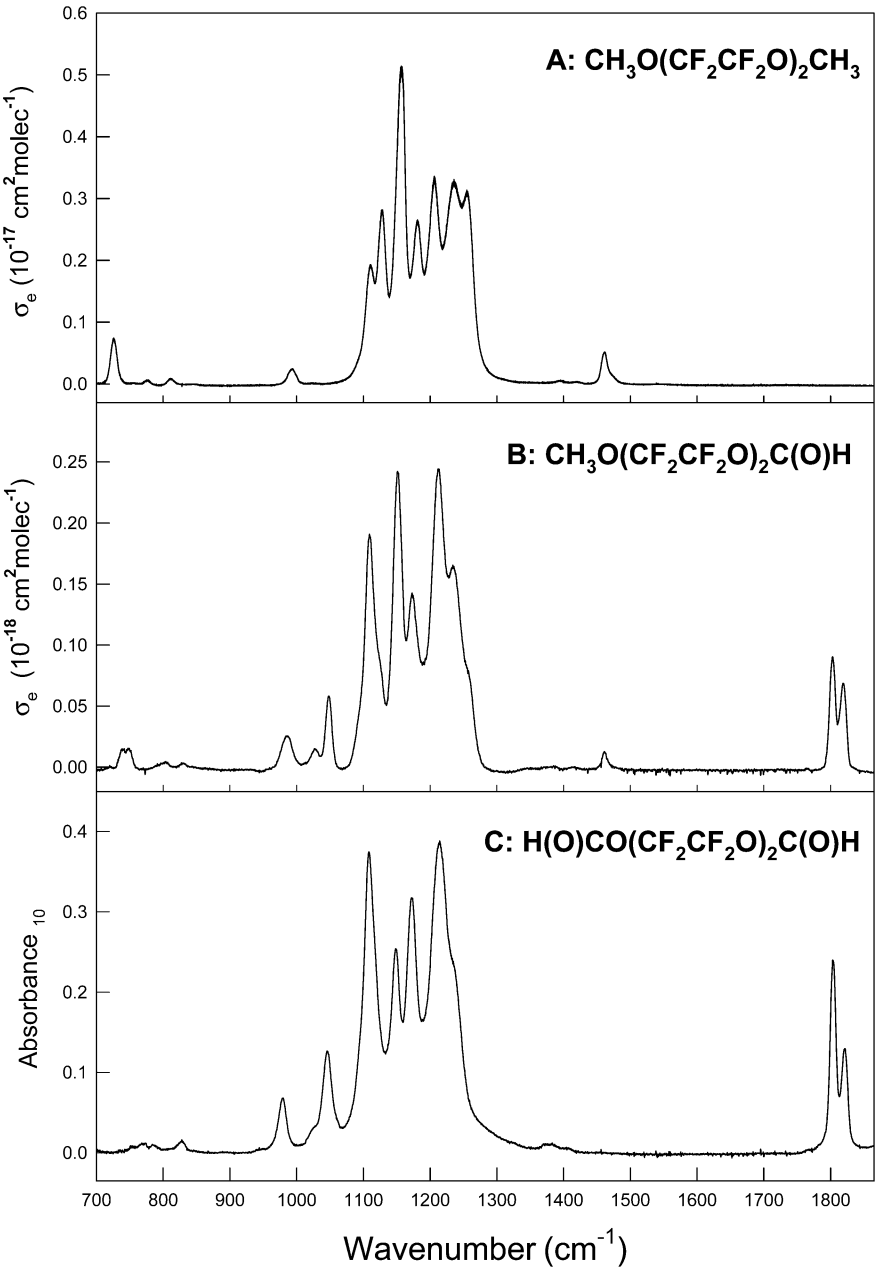

Figure 2. Infrared spectrum of $CH_3O(CF_2CF_2O)_2CH_3$ (A), $CH_3O(CF_2CF_2O)_2C(O)H$ (B), and $H(O)CO(CF_2CF_2O)_2C(O)H$ (C).

combined data, represented as a solid line, gives $k_{18}/k_{17} = 0.490 \pm 0.034$. Using $k_{17} = k_{11} = (3.7 \pm 0.7) \times 10^{-13}$ gives $k_{18} = (1.81 \pm 0.36) \times 10^{-13}$ cm^3 molecule^{-1} s^{-1}. The formate is a factor of 2 less reactive than the parent HFPE, which is attributable to the substitution of a methyl group for a formate group. Formates are significantly less reactive toward Cl atoms than the ethers from which they are derived, for example, $k(Cl + C_4F_9OCH_3)/k(Cl + C_4F_9OC(O)H) = 5$[17] and $k(Cl + CF_3OCH_3)/k(Cl + CF_3OC(O)H) = 14$.[16]

For the calibration of the $CH_3O(CF_2CF_2O)_nC(O)H$ yield in the experiments mentioned above, we assumed that $CH_3O(CF_2CF_2O)_2CH_3$ is converted into $CH_3O(CF_2CF_2O)_nC(O)H$ in essentially a 100% yield. It is possible that $CH_3O(CF_2CF_2O)_nCH_2OH$ could be formed in the peroxy radical self-reaction 14b, though no absorption features (O−H stretch) could be confirmed in the product spectra. Fluorinated alcohols are in general very reactive toward Cl atoms with rate constants of the order of $10^{-11} - 10^{-12}$ cm^3 molecule^{-1} s^{-1}. It is likely that if $CH_3O(CF_2CF_2O)_nCH_2OH$ was formed, it would react with Cl atoms in the chamber and be converted into $CH_3O(CF_2CF_2O)_nC(O)H$.

When NO is present in the reaction mixture, the $CH_3O(CF_2CF_2O)_nCH_2O(\cdot)$ radicals are formed via reaction 3a rather than 14a. Alkoxy radicals formed in the reaction of peroxy radicals with NO are produced with significant chemical activation whereas alkoxy radicals formed by the self-reaction of peroxy radicals are formed with little, or no, activation. Chemically activated alkoxy radicals can undergo prompt decomposition,[19] and hence, the fate of alkoxy radicals formed in reaction 3a may be different from that of alkoxy radicals formed in reaction 14a. To test for this possibility, experiments with reaction mixtures consisting of 4 mTorr HFPE and 100 mTorr Cl_2 were performed in the presence of NO (13 mTorr) in 700 Torr of air diluent. As seen from Figure 5, there was no discernible impact of the presence of NO on the yield of $CH_3O(CF_2CF_2O)_2C(O)H$. This observation suggests that chemical activation does not play

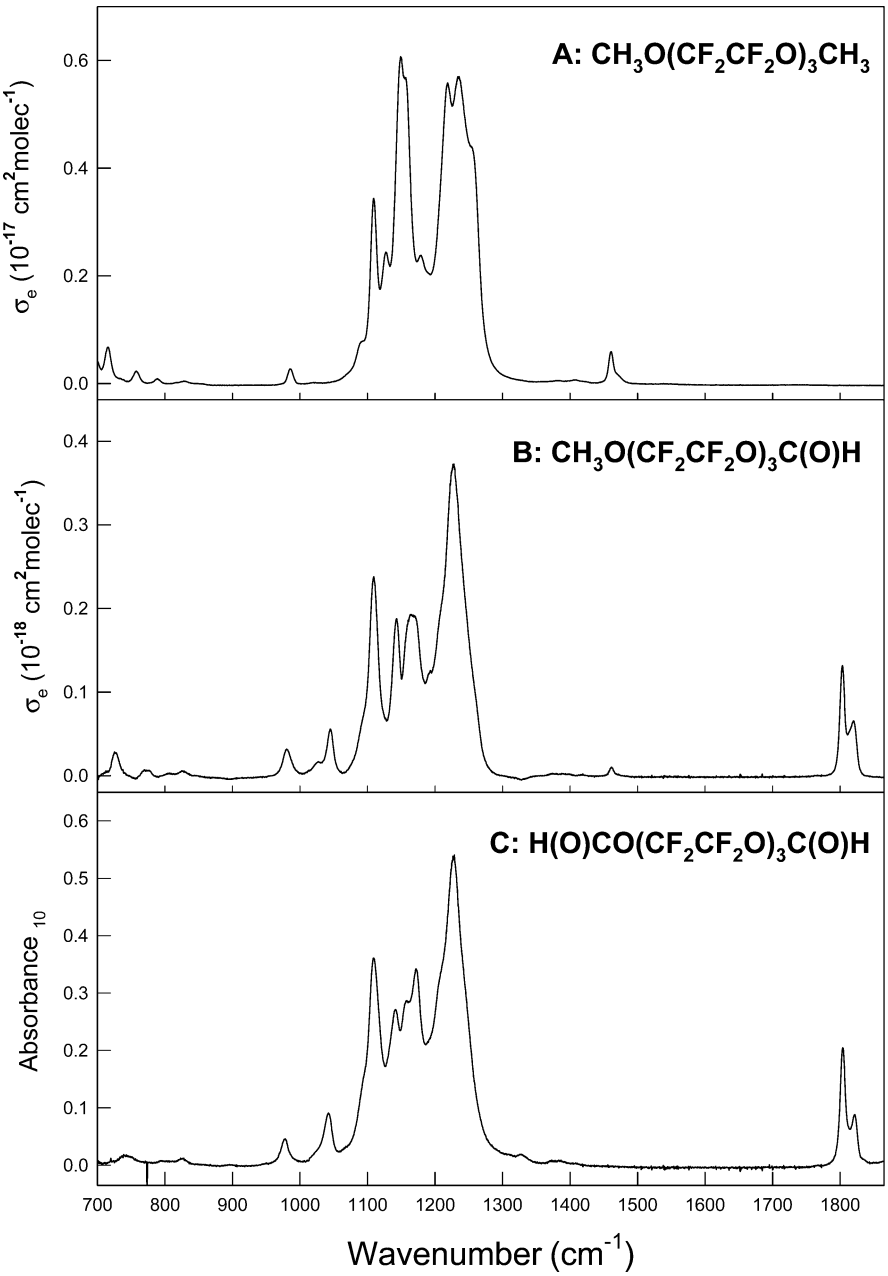

Figure 3. Infrared spectrum of $CH_3O(CF_2CF_2O)_3CH_3$ (A), $CH_3O(CF_2CF_2O)_3C(O)H$ (B), and $H(O)CO(CF_2CF_2O)_3C(O)H$ (C).

a role in the atmospheric fate of $CH_3O(CF_2CF_2O)_nCH_2O(\cdot)$ radicals.

3.3. Relative Rate Study of $k(OH + CH_3O(CF_2CF_2O)_nCH_3)$. The kinetics of reaction 1 were measured relative to reaction 19 and 20

$$CH_3O(CF_2CF_2O)_nCH_3 + OH \rightarrow \text{products} \quad (1)$$

$$C_2H_4 + OH \rightarrow \text{products} \quad (19)$$

$$C_2H_2 + OH \rightarrow \text{products} \quad (20)$$

Initial concentrations were 47−80 mTorr $CH_3O(CF_2CF_2O)_n$-CH_3, 89−101 mTorr CH_3ONO, 4.4−7.6 mTorr NO and 3.4−4.8 mTorr of either C_2H_4, or C_2H_2, in 700 Torr of air diluent. As shown by Takahashi et al.,[20] a variation of the relative rate technique can be useful when working with relatively unreactive compounds. Thus, the loss of $CH_3O(CF_2CF_2O)_nCH_3$ was not measured directly but was calculated from the observed formation of $CH_3O(CF_2CF_2O)_nC(O)H$ by assuming that the OH initiated oxidation of $CH_3O(CF_2CF_2O)_nCH_3$ gives $CH_3O(CF_2$-$CF_2O)_nC(O)H$ in a 100% molar yield. $CH_3O(CF_2CF_2O)_nCH_3$ is relatively unreactive toward OH radicals and its fractional consumption was small. To facilitate detection of $CH_3O(CF_2$-$CF_2O)_nC(O)H$ from small fractional conversions of $CH_3O(CF_2$-$CF_2O)_nCH_3$, we employed high initial concentrations of HFPE (47−80 mTorr) in the experiments.

Figure 6 shows the calculated loss of $CH_3O(CF_2CF_2O)_nCH_3$ versus the observed loss of the reference compounds, C_2H_2 and C_2H_4, when exposed to OH radicals in 700 Torr of air. Linear least-squares fits to the data for $n = 1-3$ gave values of $k_1/k_{19} = 0.0037 \pm 0.0004$, 0.0033 ± 0.0003, and 0.0032 ± 0.0003 for $n = 1-3$, respectively. Within the experimental uncertainties, there was no discernible effect of chain length on the reactivity of $CH_3O(CF_2CF_2O)_nCH_3$. The line through the composite data set obtained using C_2H_4 as a reference compound in Figure 6 has a slope of $k_1/k_{19} = 0.0035 \pm 0.0004$. The reactivity of $CH_3O(CF_2CF_2O)_2CH_3$ was measured relative to that of C_2H_2.

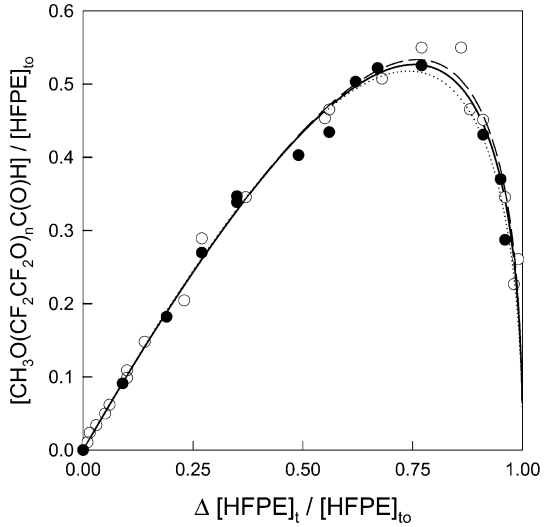

Figure 4. Plot of the observed concentration of $CH_3O(CF_2CF_2O)_nC(O)H$ ($n = 2$, open symbols; $n = 3$, solid symbols) normalized to the initial $CH_3O(CF_2CF_2O)_nCH_3$ concentration versus the fractional loss of $CH_3O(CF_2CF_2O)_nCH_3$ following irradiation of mixtures of $CH_3O(CF_2CF_2O)_nCH_3$ and Cl_2 in 700 Torr of air diluent.

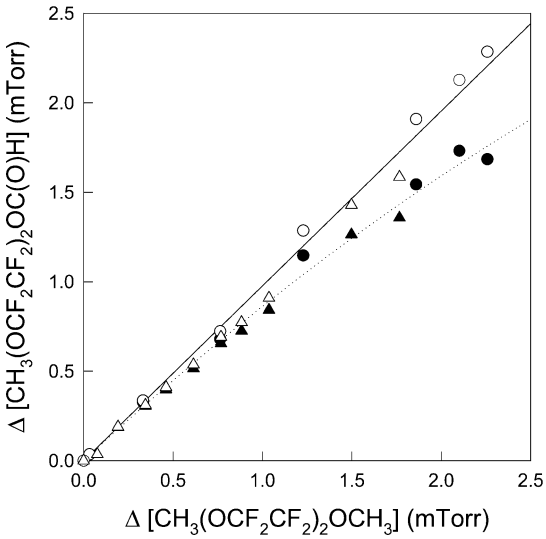

Figure 5. Formation of $CH_3O(CF_2CF_2O)_2C(O)H$ versus loss of $CH_3O(CF_2CF_2O)_2CH_3$ following Cl atom initiated oxidation of $CH_3O(CF_2CF_2O)_2CH_3$ in 700 Torr of air in the presence (triangles) or absence (circles) of NO. The open symbols show the result of correcting for loss of $CH_3O(CF_2CF_2O)_2C(O)H$ via reaction with Cl atoms (see text for details). The line is a fit through the corrected data.

The results are shown in Figure 6 which give $k_1/k_{20} = 0.0324 \pm 0.0031$. Using $k_{19} = 8.66 \times 10^{-12}$ [21] and $k_{20} = 8.45 \times 10^{-13}$ [22] gives $k_1 = (3.03 \pm 0.35) \times 10^{-14}$ and $k_1 = (2.74 \pm 0.26) \times 10^{-14}$ cm^3 molecule^{-1} s^{-1}. We choose to cite a final value for k_1, which is the average of those determined using two different reference compounds together with error limits that encompass the extremes of the individual determinations. Hence, $k_1 = (2.89 \pm 0.50) \times 10^{-14}$ cm^3 molecule^{-1} s^{-1}.

Assuming an atmospheric lifetime for methane of 9.27 years[23] and a rate constant for the $CH_4 + OH$ reaction of 6.3×10^{-15} cm^3 molecule^{-1} s^{-1} [15] leads to an estimate of the atmospheric lifetime of $CH_3O(CF_2CF_2O)_nCH_3$ with respect to reaction with OH radicals of 2 years. It is worth noting that the optimal temperature for such a scaling analysis is 272 K[24] (rather than 296 K used here) but we do not have any data for k_1 at 272 K. By analogy to similar halogenated organic compounds,[15] the temperature dependence of reaction 1 is expected to be

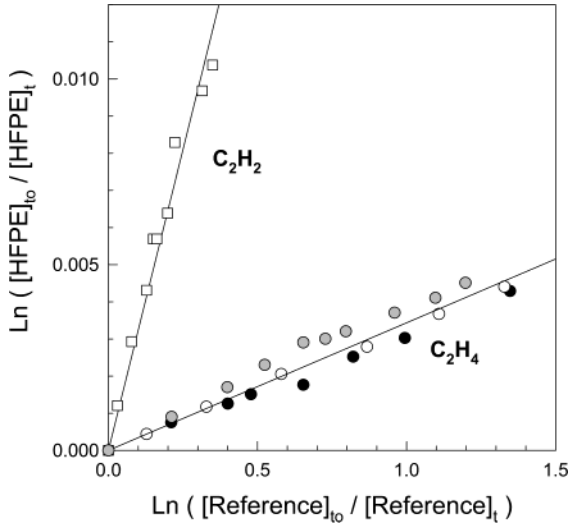

Figure 6. Decay of $CH_3O(CF_2CF_2O)_3CH_3$ (solid symbols), $CH_3O(CF_2CF_2O)_2CH_3$ (open symbols), and $CH_3OCF_2CF_2OCH_3$ (gray symbols) versus C_2H_4 (circles) and C_2H_2 (squares) in the presence of OH radicals in 700 Torr of air diluent at 296 ± 3 K.

comparable to that for reaction of OH radicals with CH_4 and in view of the small temperature difference between 296 and 272 K the use of kinetic data at 296 K should provide a reasonable estimation for the atmospheric lifetime of $CH_3O(CF_2CF_2O)_nCH_3$.

3.4. IR Spectra and Global Warming Potentials of $CH_3O(CF_2CF_2O)_nCH_3$. The IR spectra of $CH_3O(CF_2CF_2O)_nCH_3$ ($n = 1-3$) recorded at Copenhagen over the spectral range 200−1800 cm^{-1} are shown in Figure 7. The spectra in Figure 7 span a frequency range which is significantly larger than that routinely accessible by the FTIR spectrometers used at Ispra and Ford. Table 1 shows a comparison of the integrated absorption cross sections for $CH_3O(CF_2CF_2O)_nCH_3$ in the region 1060−1360 cm^{-1} measured in the three laboratories. As seen from Table 1, there is good agreement between the spectra recorded at Ispra, Ford, and Copenhagen which provides confidence in the experimental techniques used.

Using the method outlined by Pinnock et al.,[14] the IR spectra of $CH_3O(CF_2CF_2O)_nCH_3$ shown in Figure 7, and the IR spectrum of CFC-11 reported elsewhere,[25] we calculate instantaneous forcings for $CH_3O(CF_2CF_2O)_nCH_3$ ($n = 1-3$) and CFC-11 of 0.32, 0.61, 0.83, and 0.26 W m^{-2} ppb^{-1}, respectively. The following expression, as derived in the appendix, can be used to estimate values of the HGWP (halocarbon global warming potential) for $CH_3O(CF_2CF_2O)_nCH_3$ (relative to CFC-11):

$$GWP_{CFC-11basis} = \frac{IF_{HPFE}}{IF_{CFC-11}} \cdot \frac{MW_{CFC-11}}{MW_{HPFE}} \cdot \frac{\tau_{HPFE}}{\tau_{CFC-11}} \cdot \frac{(1 - e^{t/\tau_{HPFE}})}{(1 - e^{-t/\tau_{CFC-11}})}$$

where IF_{HPFE}, IF_{CFC-11}, MW_{HPFE}, MW_{CFC-11}, τ_{HFPE}, and τ_{CFC-11} are the direct instantaneous forcings, molecular weights, and atmospheric lifetimes of the two species and t is the time horizon over which the forcing is integrated. Using $\tau_{HPFE} = 2$ years and $\tau_{CFC-11} = 45$ years,[26] we estimate that the HGWPs of $CH_3O(CF_2CF_2O)_nCH_3$ ($n = 1-3$) are ≈ 0.13, 0.14, and 0.14 for a 20 year horizon and ≈ 0.051, 0.058, and 0.055 for a 100 year time horizon, respectively. The GWP of CFC-11 relative to CO_2 has been estimated on the basis of direct instantaneous forcings to be 6300 and 4600 over time horizons of 20 and 100 years, respectively. Thus, the GWP for the fluorinated ethers

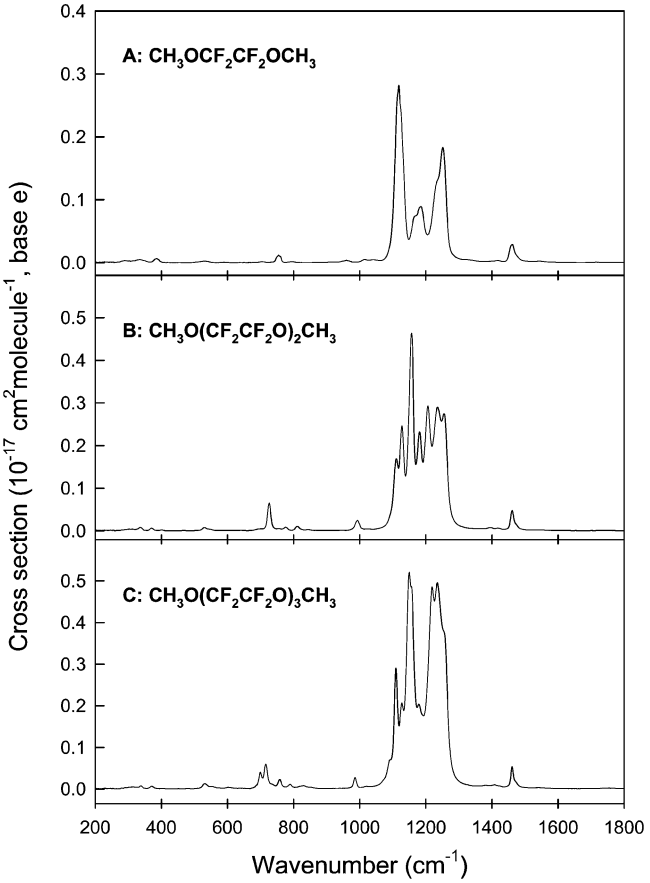

Figure 7. Infrared spectra of $CH_3OCF_2CF_2OCH_3$ (A), $CH_3O(CF_2CF_2O)_2CH_3$ (B), and $CH_3O(CF_2CF_2O)_3CH_3$ (C).

considered in the present work can be scaled accordingly, yielding GWPs (relative to CO_2) of $CH_3O(CF_2CF_2O)_nCH_3$ ($n = 1-3$) $\approx$ 820, 880, and 880 for a 20 year horizon and $\approx$ 230, 270, and 250 for a 100 year time horizon, respectively. As a result of their short atmospheric lifetimes, the fluorinated ethers considered in the present work have small GWPs and their emission into the atmosphere will not contribute significantly to radiative forcing of climate change.

4. Atmospheric Implications

We present herein a large quantity of self-consistent kinetic and mechanistic data relating to the atmospheric chemistry of $CH_3O(CF_2CF_2O)_nCH_3$ ($n = 1-3$). As expected for such structurally similar molecules, their atmospheric chemistry is indistinguishable. It seems reasonable to generalize our results to include all molecules where the general formula is $CH_3O(CF_2CF_2O)_nCH_3$ ($n \geq 1$).

The atmospheric lifetime of $CH_3O(CF_2CF_2O)_nCH_3$ will be determined by reaction with OH radicals. In the present work, we report $k(OH + CH_3O(CF_2CF_2O)_nCH_3) = (2.9 \pm 0.5) \times 10^{-14}$ cm^3 molecule^{-1} s^{-1}. In addition to reaction with OH radicals, organic compounds are removed from the atmosphere via photolysis, wet deposition, dry deposition, and reaction with NO_3 radicals, Cl atoms, and O_3. For saturated compounds such as $CH_3O(CF_2CF_2O)_nCH_3$, reaction with NO_3 radicals and O_3 are typically too slow to be of importance. The average concentration of Cl atoms in the troposphere is orders of magnitude less than that of OH radicals.[27] In the present study, we observe that Cl atoms are 13 times more reactive than OH radicals toward $CH_3O(CF_2CF_2O)_nCH_3$. Reaction with Cl atoms will not be a significant atmospheric loss mechanism for $CH_3O(CF_2CF_2O)_nCH_3$. Ethers do not absorb at UV wavelengths >200 nm.[28] Hence, photolysis of $CH_3O(CF_2CF_2O)_nCH_3$ will not be important in the troposphere. Highly fluorinated molecules such as $CH_3O(CF_2CF_2O)_nCH_3$ are hydrophobic and wet deposition is unlikely to be of importance. Finally, at least for the smaller members of the $CH_3O(CF_2CF_2O)_nCH_3$ group, the volatility of these compounds will render dry deposition an unlikely removal mechanism. In conclusion, the atmospheric lifetime of $CH_3O(CF_2CF_2O)_nCH_3$ is determined by reaction with OH and is approximately 2 years.

As shown herein, the OH initiated oxidation of $CH_3O(CF_2CF_2O)_nCH_3$ gives the formate $CH_3O(CF_2CF_2O)_nC(O)H$. The formate reacts with Cl atoms at a rate which is approximately half of that of the parent ether. The simplest explanation of this observation is that the $-C(O)H$ group is substantially less reactive than the $-OCH_3$ group in $CH_3O(CF_2CF_2O)_nC(O)H$. It seems likely that the reactivity of OH radicals toward the formate $CH_3O(CF_2CF_2O)_nC(O)H$ will also be approximately half of that of the parent ether $CH_3O(CF_2CF_2O)_nCH_3$. Additional loss mechanisms for the formate such as photolysis, hydrolysis, and dry deposition may be important. Further research is needed to quantify the rates of such processes.

With regard to the environmental impact of $CH_3O(CF_2CF_2O)_nCH_3$, we can make the following statements. First, $CH_3O(CF_2CF_2O)_nCH_3$ does not contain any chlorine and will not contribute to stratospheric ozone depletion via the well-established chlorine based chemistry. As with all hydrofluorocarbons (HFCs) and hydrofluoroethers (HFEs), the ozone depletion potential of $CH_3O(CF_2CF_2O)_nCH_3$ is zero. Second, the atmospheric lifetime of $CH_3O(CF_2CF_2O)_nCH_3$ is approximately 2 years, and consequently, these compounds have small GWPs as described herein. Third, the atmospheric oxidation of $CH_3O(CF_2CF_2O)_nCH_3$ gives the fluorinated formate $CH_3O(CF_2CF_2O)_nC(O)H$. The formate is not expected to be persistent or pose any significant environmental hazard. Additional study of the environmental fate of the formate would be useful to provide a more complete picture of the atmospheric degradation mechanism of $CH_3O(CF_2CF_2O)_nCH_3$.

Acknowledgment. M.P.S.A. thanks the Danish Research Agency for a research grant.

5. Appendix

The global warming potential (GWP) of a substance is defined as the ratio of the time-integrated radiative forcing from the instantaneous release of 1 kg of the substance relative to that of 1 kg of a reference gas

$$\mathrm{GWP} = \frac{\int_0^t a_x[x(t)]\,\mathrm{d}t}{\int_0^t a_r[r(t)]\,\mathrm{d}t} \qquad \text{(a)}$$

where t is the time horizon over which the calculation is considered, a_x (or a_r) is the radiative efficiency due to a unit increase in atmospheric abundance of the substance in question (units of W m^{-2} kg^{-1}), and $[x(t)]$ and $[r(t)]$ are the time-dependent concentrations of the substance and reference.

CFC-11 is a convenient reference compound, hence

$$\mathrm{GWP}_{\mathrm{CFC-11basis}} \equiv \mathrm{HGWP}(x) = \frac{\int_0^t a_x[x(t)]\,\mathrm{d}t}{\int_0^t a_{\mathrm{CFC-11}}[\mathrm{CFC\text{-}11}(t)]\,\mathrm{d}t} \qquad \text{(b)}$$

We define $[x(t)]$ as $[x(t)] \equiv \mathrm{e}^{-t/\tau_x}$ and $[\mathrm{CFC\text{-}11}(t)] \equiv \mathrm{e}^{-t/\tau_{\mathrm{CFC-11}}}$,

where τ is the atmospheric lifetime. Substituting these expressions into eq b gives

$$\mathrm{GWP}_{\mathrm{CFC-11basis}} = \frac{a_x}{a_{\mathrm{CFC-11}}} \cdot \frac{\int_0^t \mathrm{e}^{-t/\tau_x}\,\mathrm{d}t}{\int_0^t \mathrm{e}^{-t/\tau_{\mathrm{CFC-11}}}\,\mathrm{d}t} = \frac{a_x}{a_{\mathrm{CFC-11}}} \cdot \frac{(-\tau_x \mathrm{e}^{-t/\tau_x})|_0^t}{(-\tau_{\mathrm{CFC-11}}\mathrm{e}^{-t/\tau_{\mathrm{CFC-11}}})|_0^t}$$

$$\mathrm{GWP}_{\mathrm{CFC-11basis}} = \frac{a_x}{a_{\mathrm{CFC-11}}} \frac{(-\tau_x \mathrm{e}^{t/\tau_x} + \tau_x)}{(-\tau_{\mathrm{CFC-11}}\mathrm{e}^{-t/\tau_{\mathrm{CFC-11}}} + \tau_{\mathrm{CFC-11}})}$$

$$\mathrm{GWP}_{\mathrm{CFC-11basis}} = \frac{a_x}{a_{\mathrm{CFC-11}}} \frac{\tau_x}{\tau_{\mathrm{CFC-11}}} \frac{(1 - \mathrm{e}^{t/\tau_x})}{(1 - \mathrm{e}^{-t/\tau_{\mathrm{CFC-11}}})} \quad \text{(c)}$$

Values of a_x and $a_{\mathrm{CFC-11}}$ have units of W m^{-2} kg^{-1} and can be calculated from IR absorption spectra of x and CFC-11. More typically, spectral data such as those shown in Figure 7 are used to calculate instantaneous forcings (IF) in units of W m^{-2} ppb^{-1} caused by a 1 ppb increase in atmospheric concentration of the compound.[14] As GWP is defined on a mass basis, the molecular weights (MW) of each substance must be taken into account when operating with IFs, thus

$$\mathrm{GWP}_{\mathrm{CFC-11basis}} = \frac{\mathrm{IF}_x}{\mathrm{IF}_{\mathrm{CFC-11}}} \frac{\mathrm{MW}_{\mathrm{CFC-11}}}{\mathrm{MW}_x} \frac{\tau_x}{\tau_{\mathrm{CFC-11}}} \frac{(1 - \mathrm{e}^{t/\tau_x})}{(1 - \mathrm{e}^{-t/\tau_{\mathrm{CFC-11}}})} \quad \text{(d)}$$

References and Notes

(1) Molina, M. J.; Rowland, F. S. *Nature* **1974**, *249*, 810.

(2) Farman, J. D.; Gardiner, B. G.; Shanklin, J. D. *Nature* **1985**, *315*, 207.

(3) Marchionni, G.; Visca, M. *Eur. Pat. Appl., 1275678A*, 2003, (Chem. Abs. 138, 90675).

(4) Sianesi, D.; Marchionni, G.; De Pasquale, R. J. In *Organofluorine Chemistry: Principles and Commercial Applications*; Banks, R. E., Ed.; Plenum Press: New York, 1994.

(5) Marchionni, G.; Ajroldi, G.; Pezzin, G. In *Comprehensive Polymer Science*, Second Supplement; Agarwal, S. L., Russom, S., Eds.; Pergamon: London, 1996.

(6) Marchionni, G.; Guarda, P. A. U.S. Patent, 5,744,651, 1998.

(7) Marchionni, G.; Maccone, P.; Pezzin G. *J. Fluor. Chem.* **2002**, *118*, 149.

(8) Wallington, T. J.; Schneider, W. F.; Worsnop, D. R.; Nielsen, O. J.; Sehested, J.; Debruyn, W. J.; Shorter, J. A. *Environ. Sci. Technol*. **1994**, *28*, 320A.

(9) Tyndall, G. S.; Cox, R. A.; Granier, C.; Lesclaux, R.; Moortgat, G. K.; Pilling, M. J.; Ravishankara, A. R.; Wallington, T. J. *J. Geophys. Res. D* **2001**, *106*, 12157.

(10) Wallington, T. J.; Japar, S. M. *J. Atmos. Chem*. **1989**, *9*, 399.

(11) Ballesteros, B.; Jensen, N. R.; Hjorth, J. *J. Atm. Chem.* **2002**, *43*, 135−150.

(12) Atkinson, R. *J. Phys. Chem. Ref. Data* **1989**, Monograph 1.

(13) Nielsen, O. J.; Sidebottom, H. W.; Donlon, M.; Treacy, J. *Int. J. Chem. Kinet.* **1991**, *23*, 1095.

(14) Pinnock, S.; Hurley, M. D.; Shine, K. P.; Wallington, T. J.; Smyth, T. J. *J. Geophys. Res.* **1995**, *100*, 23227.

(15) Sander, S. P.; Friedl, R. R.; Golden, D. M.; Kurylo, M. J.; Huie, R. E.; Orkin, V. L.; Moortgat, G. K.; Ravishankara, A. R.; Kolb, C. E.; Molina, M. J.; Finlayson-Pitts, B. J. *J. JPL Publ.* **2003**, *02*−*25*.

(16) Christensen, L. K.; Wallington, T. J.; Gushin, A.; Hurley, M. D. *J. Phys. Chem. A* **1999**, *103*, 4202.

(17) Wallington, T. J.; Schneider, W. F.; Sehested, J.; Bilde, M.; Nielsen, O. J.; Christensen, L. K.; Molina, M. J.; Molina, L. T.; Wooldridge, P. W. *J. Phys. Chem. A* **1997**, *101*, 8264.

(18) Meagher, R. J.; McIntosh, M. E.; Hurley, M. D.; Wallington, T. J. *Int. J. Chem. Kinet.* **1997**, *29*, 619.

(19) Wallington, T. J.; Hurley, M. D.; Fracheboud, J. M.; Orlando, J. J.; Tyndall, G. S.; Sehested, J.; Møgelberg, T. E.; Nielsen O. J. *J. Phys. Chem.* **1996**, *100*, 18116.

(20) Takahashi, K.; Matsumi, Y.; Wallington, T. J.; Hurley, M. D. *J. Geophys. Res. D* **2002**, *107*, ACH 4-1.

(21) Calvert, J. G.; Atkinson, R.; Kerr, J. A.; Madronich, S.; Moortgat, G. K.; Wallington, T. J.; Yarwood, G. *The Mechanism of Atmospheric Oxidation of the Alkenes*; Oxford University Press: New York, 2000.

(22) Sørensen, M.; Kaiser, E. W.; Hurley, M. D.; Wallington, T. J.; Nielsen, O. J. *Int. J. Chem. Kinet*. **2003**, *35*, 191.

(23) Prinn R. G.; Huang, J.; Weiss R. F.; Cunnold, D. M.; Fraser, P. J.; Simmonds, P. G.; McCulloh, A.; Harth, C.; Salameh, P.; O'Doherty, S.; Wang, R. H. J.; Porter, L.; Miller, B. R. *Science* **2001**, *292*, 1882.

(24) Spivakovsky, C. M.; Logan, J. A.; Montzka, S. A.; Balkanski, Y. L.; Foreman-Fowler, M.; Jones, D. B. A.; Horowitz, L. W.; Fusco, A. C.; Brenninkmeijer, C. A. M.; Prather, M. J.; Wofsy, S. C.; McElroy, M. B. *J. Geophys. Res. D* **2000**, *105*, 8931.

(25) Ninomiya, Y.; Kawasaki, M.; Gushin, A.; Molina, L. T.; Molina, M.; Wallington, T. J. *Environ. Sci. Technol*. **2000**, *34*, 2973.

(26) Houghton, J. T.; Ding, Y.; Griggs, D. J.; Noguer, M.; van der Linden, P. J.; Dai, X.; Maskell, K.; Johnson, C. A. Climate Change 2001: The Scientific Basis, *Intergovernmental Panel on Climate Change*; Cambridge University Press: New York, 2001.

(27) Finlayson-Pitts, B. J.; Pitts, J. N., Jr. *Atmospheric Chemistry: Fundamentals and Experimental Techniques*; John Wiley and Sons: New York, 1986.

(28) Calvert, J. G.; Pitts, J. N., Jr. *Photochemistry*; John Wiley: New York, 1966.